Check for updates

Kinetics of photocatalytic degradation of organic compounds: a mini-review and new approach†

Hai D. Tran, [ID] [a] Dinh Quan Nguyen, [ID] *[bc] Phuong T. Do*[d] and Uyen N. P. Tran [ID] *[e]

Organic compounds are widespread pollutants in wastewater, causing significant risks for living organisms. In terms of advanced oxidation processes, photocatalysis is known as an effective technology for the oxidation and mineralization of numerous non-biodegradable organic contaminants. The underlying mechanisms of photocatalytic degradation can be explored through kinetic studies. In previous works, Langmuir–Hinshelwood and pseudo-first-order models were commonly applied to fit batch-mode experimental data, revealing critical kinetic parameters. However, the application or combination conditions of these models were inconsistent or ignored. This paper briefly reviews kinetic models and various factors influencing the kinetics of photocatalytic degradation. In this review, kinetic models are also systemized by a new approach to establish a general concept of a kinetic model for the photocatalytic degradation of organic compounds in an aqueous solution.

[a]Faculty of Environment, Ho Chi Minh University of Natural Resources and Environment, Ho Chi Minh City, Vietnam

[b]Laboratory of Biofuel and Biomass Research, Faculty of Chemical Engineering, Ho Chi Minh City University of Technology (HCMUT), 268 Ly Thuong Kiet, District 10, Ho Chi Minh City, Vietnam. E-mail: ndquan@hcmut.edu.vn

[c]Vietnam National University Ho Chi Minh City, Linh Trung Ward, Thu Duc District, Ho Chi Minh City, Vietnam

[d]Office of R&D and External Relations, Ho Chi Minh University of Natural Resources and Environment, Ho Chi Minh City 70000, Vietnam. E-mail: dtphuong@hcmunre.edu.vn

[e]Faculty of Engineering and Technology, Van Hien University, Ho Chi Minh City, Vietnam. E-mail: uyentpn@vhu.edu.vn

† Electronic supplementary information (ESI) available. See DOI: https://doi.org/10.1039/d3ra01970e

Introduction

Studies on wastewater treatment have focussed on developing sustainable and suitable technologies for removing organic pollutants since many detected organic compounds interact with biological systems, raising concerns about potential human exposure and ecological health.[1,2] Today, there are various methods for the degradation of organic compounds, such as wet oxidation,[3] biological oxidation,[4] electrochemical redox,[5] advanced oxidation processes (AOPs)[6] or combined process.[7] AOPs, including photocatalysis, are considered high efficiency for degrading organic compounds in water.[8,9] By generating reactive species, such as hydroxyl radicals (˙OH),

MsC. Hai D. Tran received his Master of Science degree in Chemistry from Ho Chi Minh University of Technology (HCMUT) in 2014. He is working for Ho Chi Minh University of Natural Resources and Environment (HCMUNRE), Vietnam. He is currently a master of materials science, chemical engineering, and modeling. His research has focused on the development of new materials for a variety of applications, including waste-to-energy, environmental treatment, sensors, and catalysis. He was also a leader in many scientific research projects in Vietnam. He is active and responsible. He has published several high-quality papers.

Assoc. Prof. Dr Dinh Quan Nguyen earned his PhD in 2008 from Korea Insititute of Science and Technology (KIST). Presently, he serves as the Head of the Laboratory of Biofuel and Biomass Research at Ho Chi Minh University of Technology (HCMUT), which is part of Vietnam National University Ho Chi Minh City (VNU-HCM). Dr Ng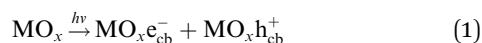uyen has an extensive research background and has published over 50 scientific papers encompassing various topics such as renewable energy, biomass, and secondary batteries. His work contributes significantly to the advancements in these fields, offering valuable insights and innovations.

with an oxidation potential of 2.8 eV,[10] AOPs are known as strong oxidation processes with the complete mineralization capability of organic pollutants.[8]

Recently, many studies on the photocatalytic oxidation process focused on developing it by understanding its mechanisms and kinetics. As in a principle of this route, hydroxyl radical $^\cdot$OH is formed on a photo-excited catalyst's surface under appropriate illumination, typically for UV radiation. Generally, a photocatalytic mechanism for organic degradation using a metal oxide catalyst (MO_x) was described as a chain of reactions from (1) to (4).[11,12]
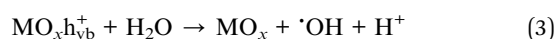
Photo-excitation:

$$MO_x \xrightarrow{hv} MO_x e_{cb}^- + MO_x h_{cb}^+ \tag{1}$$

Recombination:

$$MO_x e_{cb}^- + MO_x h_{cb}^+ \rightarrow MO_x + heat \tag{2}$$

Hydroxyl radical formation:

$$MO_x h_{vb}^+ + H_2O \rightarrow MO_x + {}^\cdot OH + H^+ \tag{3}$$

Degradation reaction:

$$^\cdot OH + P \rightarrow Q \tag{4}$$

P is an organic compound, Q represents a product. e_{cb}^- is electron in the conduction band, h_{vb}^- is hole in the valence band.

As photocatalytic degradation (PCD) reactions occur at the interfaces, most photocatalyzed oxidations in water involve $^\cdot$OH radicals, considered the primary oxidizer to degrade organic compounds.[13] However, the lifetime of $^\cdot$OH in water is only several microseconds.[14] Therefore, organic compounds are majorly degraded at photo-excited catalyst surface where $^\cdot$OH was carried. Kinetic studies of PCD of organic compounds have been presented in the literature and provided specific evidence to understand PCD mechanism and performance. This paper aims to briefly review the kinetic models of PCD in progress, in which the Langmuir–Hinshelwood and the pseudo-order kinetic models are emphasized to analyze. In heterogeneous catalytic reactions, the use of appropriate kinetic models is crucial. These two models are reliable kinetic candidates for predicting mechanism and catalytic performances, which has been the subject of previous extensive analysis. This review also proposes a new approach to systemizing the PCD kinetic models that contribute to optimizing and implementing this wastewater treatment method.

The Langmuir–Hinshelwood model

Langmuir–Hinshelwood (L–H) mechanism was used for characterizing solid catalytic reactions,[15] which consists of four steps: (1) adsorption of molecules on a catalytic surface, (2) dissociation of adsorbed molecules, (3) reactions of dissociated molecules to produce products, and (4) desorption of products.[16] This model has been reported for the heterogeneous catalytic degradation of organic wastewater.

According to step 1, the rate of adsorption and desorption are expressed as eqn (5) and (6).[17]

$$r_a = k_a(1 - \theta)C_P \tag{5}$$

$$r_d = k_d \theta \tag{6}$$

where k_a and k_d are an adsorption and desorption rate constant, θ is a fraction of the coverage site, and C_P is a concentration of P in a medium.

MsC Phuong T. Do earned her Master's degree in 2016 from the Industrial University of Ho Chi Minh City (IUH). Presently, she serves as the specialist of the Office of Research Development and External Relations at Ho Chi Minh City University of Natural Resources and Environment (HCMUNRE), which is operated directly under the authority of the Ministry of Natural Resources and Environment (MONRE). She has extensive expertise contributing to research in the fields of chemistry, materials and catalysts, as well as the application of expertise in environmental remediation. She has also participated as a researcher in ministerial-level projects and state-level projects and has long experience in management work and group activities.

Dr Uyen P. N. Tran is currently a Lecturer and Researcher at Van Hien University, Vietnam. She obtained an Engineering Bachelor and a Master's degree from Ho Chi Minh University of Technology, Vietnam (HCMUT). Her master's focused on Metal–Organic Framework (MOF) catalysts for organic synthesis. Then, Uyen had a three year-working experience on a Biomass Conversion project collaborated by HCMUT, University of Tokyo, and JICA-JST, which promoted A Sustainable Integration of Local Agriculture and Biomass Industry. In 2015, Uyen received a University International Postgraduate Award to take her PhD at UNSW, Australia. Her PhD thesis focused on developing novel organic synthesis using sustainable methods, published in high-impact journals. After PhD graduation in 2019, she returned to Vietnam to continue chasing catalysis-based sustainable chemistry and biomass waste valorization.

At equilibrium, $r_a = r_d$, which results in eqn (7).[17,18]

$$\theta = \frac{KC_P}{1 + KC_P} \tag{7}$$

where $K = \dfrac{k_a}{k_d}$ is the adsorption equilibrium constant.

It is noted that organic molecule (P) is adsorbed before PCD. Therefore, the degradation rate is proportional to θ as eqn (8).[19]

$$r_{deg} = k_{deg}\theta = \frac{k_{deg}KC_P}{1 + KC_P} \tag{8}$$

with k_{deg} as the degradation constant.

According to the rate law of chemical reaction, the rate of P degradation is also expressed as follows:

$$r_{deg} = -\frac{dC_P}{dt} \tag{9}$$

Combining (8) and (9), eqn (10) is obtained, which is known as L–H kinetic model.[20]

$$-\frac{dC_P}{dt} = \frac{k_{deg}KC_P}{1 + KC_P} \tag{10}$$

To determine constants in eqn (10), this equation is integrated from $C_P = C_{P,0}$ at $t = 0$ to C_P at the interval time t:

$$\frac{1}{k_{deg}K}\ln\frac{C_P}{C_{P,0}} + \frac{1}{k_{deg}}(C_P - C_{P,0}) = -t \tag{11}$$

Or rearranging as (12).

$$\frac{-t}{C_P - C_{P,0}} = \frac{1}{k_{deg}} + \frac{1}{k_{deg}K}\frac{\ln(C_P/C_{P,0})}{C_P - C_{P,0}} \tag{12}$$

Linear plot $\dfrac{-t}{C_P - C_{P,0}}$ *vs.* $\dfrac{\ln(C_P/C_{P,0})}{C_P - C_{P,0}}$ generates $\dfrac{1}{k_{deg}}$ as intercept and $\dfrac{1}{k_{deg}K}$ as slope.[21]

The L–H model is well-compatible with experimental kinetic data for PCD in previous reports. Irani *et al.* studied PCD of methylene blue with ZnO nanoparticles, finding that the L–H model was better to fit the experimental data in comparison to other models.[22] The kinetic model for PCD of 2-chlorophenol with TiO$_2$ corresponds to the L–H model with a high correlation coefficient ($R^2 = 0.987$).[23] Shaik Basha *et al.* performed PCD of amoxicillin using activated carbon-supported TiO$_2$ nanoparticles as integrated photocatalytic adsorbents.[24] They found that the L–H model exhibited a better fit than first-order kinetics. Lin *et al.* also indicated the critical application of the L–H model for kinetic analysis of PCD of acid orange 7 using ordered mesoporous TiO$_2$ supported on carbon fiber.[25] However, the synergetic effect can not be explored from the L–H model.

Some aspects are inadequate in applying the L–H model for PCD.[19,26,27] Accordingly, two following prominent notes are recommended to consider:

(i) The L–H model was established based on the Langmuir adsorption mechanism, in which adsorption and desorption were considered. But the photocatalytic mechanism is beyond that of L–H mechanism.[26] If the rate of chemical reactions of adsorbed molecules on the catalyst surface is speedy, the assumed adsorption–desorption equilibrium in L–H mechanism is violated.[28]

(ii) In the L–H mechanism, the amount of active sites on a solid surface is assumed to be unchanged, which is difficult to accept for photocatalytic processes. The rate of PCD is expected to increase along with increasing photo-excited site number, which is considered a function of radiation intensity at the photocatalyst surface.[29,30] In the case of photocatalysis performance in an aqueous solution, the concentration of organic compound(s) decreases with prolonged PCD time, assigning a contribution to the variation of light absorbance of the solution.[31,32] Consequently, the photo-excited site number varies *vs.* time, significantly concerning the colored organic solution.

The pseudo-order kinetic model

To illustrate the kinetic mechanism for the degradation of an organic pollutant in the solution, the pseudo-order model was used to investigate the PCD rate. Overall, if there is the only variation of organic pollutant's concentration *vs.* time, the rate of PCD can be expressed as (13).

$$r_P = -\frac{dC_P}{dt} = k_n C_P^n \tag{13}$$

where n is reaction order, typically in the range $0 \leq n \leq 2$.[26]

(i) For $n = 1$. The integral form of (13) is a well-known pseudo-first-order (PFO) kinetic model, as presented in eqn (14).

$$C_P = C_{P,0}\exp(-k_1 t) \tag{14}$$

with k_1 as the first-order rate constant.

Eqn (14) can be rewritten to a linear form (15), revealing the $-k_1$ value as the slope of a straight line of $\ln\dfrac{C_P}{C_{P,0}}$ *vs.* t.

$$\ln\frac{C_P}{C_{P,0}} = -k_1 t \tag{15}$$

The PFO model was appropriate for fitting PCD data in some previous works.[33–39] Peters *et al.* reported PCD of rhodamine B using TiO$_2$ supported in ceramic.[40] This study demonstrated that kinetic data obeyed the PFO model by fitting eqn (15) with the contact time, revealing a high correlation coefficient ($R^2 = 0.9923$). Investigating PCD for ofloxacin using Mn-doped CuO photocatalyst, Liu *et al.* showed that the PFO model exhibited good compliance with experimental results ($R^2 = 0.9813$).[41] Another kinetic study by Gharbani *et al.* for PCD of methylene blue using CdSe nanoparticles presented a good fit of experimental result with the PFO model.[42] Also studying UV-assisted photocatalytic degradation of methylene blue, Kumar and co-workers recently investigated the PCD kinetics controlled under three different manners (UV/TiO$_2$, UV/H$_2$O$_2$, and UV/

TiO$_2$/H$_2$O$_2$) which followed an apparent PFO rate kinetics.[38] For tetracycline, the PFO model is also compatible with describing the PCD kinetic on Cu$_3$P nanoparticles/hollow tubular carbon nitride,[43] the photo-Fenton degradation on ultrathin porous g-C$_3$N$_4$.[44]

The rate constant k_1 in eqn (14) depends on reaction temperature and the chemical thermodynamic properties of subtracts.[45–47] However, several experimental parameters also affected the k_1 value.[48–50] Rytwo and Zelkind reported that heterogenous and homogenous photocatalysis could effectively degrade ofloxacin when they studied the evaluation of kinetic pseudo-order in the TiO$_2$-photocatalyzed degradation of ofloxacin.[49] Mahmoud and co-workers proved the photocatalytic degradation of methyl red dye by SiO$_2$ NPs doped with deposited surface particles.[50] The primary role of these particles affected the photocatalytic efficiency of the SiO$_2$ NPs and, consequently, changed the rate of methyl red degradation.

Generally, PCD rate depends on initial photocatalyst concentration, photocatalytic particle size, initial subtracts concentration, and light intensity. Therefore, modification of the PFO model was recommended.

(ii) For $n \neq 1$. Integrating eqn (13) yields a general expression (16).

$$C_P^{1-n} - C_{P,0}^{1-n} = k_n(n-1)t \tag{16}$$

If $C_P = \frac{1}{2}C_{P,0}$, it takes a half-life time ($t_{1/2}$)

$$t_{1/2} = \frac{2^{n-1} - 1}{(n-1)k_n}C_{P,0}^{1-n} \tag{17}$$

Eqn (17) reveals two cases: (i) $t_{1/2}$ decrease with increasing $C_{P,0}$ for $n > 1$, and (ii) $t_{1/2}$ increase with increasing $C_{P,0}$ for $n < 1$. Rytwo and Zelkind[49] explored that the $t_{1/2}$ of PCD of ofloxacin decreased with an increasing initial concentration of ofloxacin, contracting to PCD of caffeine[51] or phenol.[52]

Generally, the value of n is a real number.[53] However, most reports introduced n as an integer number without explanations. For $n = 2$, the eqn (16) is rewritten as (18), known as pseudo-second-order (PSO) kinetic, with a linear relationship between $\frac{1}{C_P}$ and t.

$$\frac{1}{C_P} - \frac{1}{C_{P,0}} = k_2 t \tag{18}$$

where k_2 is the second-order rate constant.

Only several reports have shown a well-suitable application of the PSO model for the PCD to date.[54–58] For example, the calculation in the Ernawati group's report indicated that experimental data from PCD of methylene blue on CaTiO$_3$ photocatalyst exhibit good compliance with the PSO kinetic model.[54] The compliance with this model promoted chemical sorption between adsorbent and adsorbate involving valence forces through sharing or exchanging electrons, bringing about a non-equilibrium of adsorption and desorption.[59]

Reciprocity between the L–H model and pseudo-order kinetic model

Considering eqn (10), if we set $k_{ap} = \frac{k_{deg}K}{1 + KC_P}$, this equation can be rewritten as (19).

$$-\frac{dC_p}{dt} = k_{ap}C_P \tag{19}$$

Eqn (19) is similar to (13) with $n = 1$. However, differing from an unchangeability of k_1 value, k_{ap} depends on time over a relationship of $C_P \sim t$. Therefore, the L–H model and PFO model can be considered uniform in the case:

(i) Variation of C_P is a faint effect on k_{ap}. At a low range of C_P, the term of $KC_P \ll 1$, and $k_{ap} \approx k_{deg}K = k_1$ is a constant. The L–H model is simplified to the PFO model in which substrate concentration is less than 10^{-3} mol L^{-1}.[60]

(ii) The L–H model is applied for the initial stage of photodegradation. In this case, k_{ap} depends on $C_{P,0}$ revealing the relationship (20). A linear form of eqn (20) is expressed by (21) and is commonly applied in numerous studies.[33,61–63]

$$k_1 = \frac{k_{deg}K}{1 + KC_{P,0}} \tag{20}$$

$$\frac{1}{k_1} = \frac{1}{k_{deg}K} + \frac{1}{k_{deg}}C_{P,0} \tag{21}$$

If $KC_P \ll 1$ then $1 + KC_P \approx KC_P$ and eqn (10) becomes $-\frac{dC_P}{dt} = k_{deg}$, which matches to (13) with $n = 0$ (pseudo-zero-order model).[64] Moreover, there is no clear reciprocity principle between the L–H model and another pseudo-order kinetic model mentioned in the previous works.

## Effect of various factors on photocatalytic degradation kinetics

Effect of light intensity

Several factors significantly affect the PCD of organic compounds, including light intensity.[65] The radiation intensity is attenuated due to light absorption of suspension, accounting for photocatalyst concentration, medium and contaminants concentration.[66] For $d_p/\lambda \ll 0.1$, the light absorption due to particulate dispersions is described by extinction eqn (22).[67] For each PCD experiment, the photocatalyst concentration in suspension can be assumed to be unchanged, suggesting I_S as a constant.

$$I_S = I_0 10^{-\mu_S C_S} \tag{22}$$

where I_0 is the intensity of incident light, μ is attenuation coefficient, C_S is the concentration of particle in suspension.

Contaminants in solution may play a significant cause in the attenuation of light intensity, especially for colored organic compounds.[66] Ollis *et al.* estimated that 46% to 99% of UV light
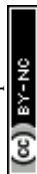
(254 nm) was absorbed in solophenyl green BE solution in a range of concentration from 5 to 50 mg L^{-1}.[62] In comparison to the anion dye solution, UV light absorbance of several cation dye solutions is higher.[68] According to Beer–Lambert law, the UV intensity at a catalyst surface relates to the concentration of dissolved contaminants as eqn (23).[69]

$$I_P = I_0 10^{-\mu_P C_P} \tag{23}$$

Therefore, light intensity at photocatalyst in PCD is expressed as (24).

$$I_a = I_0 10^{-\mu_S C_S - \mu_P C_P} \tag{24}$$

And the total absorbance caused by particles and dissolved contaminants is expressed as (25).

$$A = A_S + A_P = \mu_S C_S + \mu_P C_P \tag{25}$$

It notes that C_P in eqn (23) decreases with the increasing contact time due to degradation, resulting in I_a as a function of time. In the case of the faint effect of organic compounds' presence on the solution's light absorption, I_a can be considered a constant. An example of this case is a low range of initial concentration of orange G (<40 ppm).[21] Oppositely, the dependence of rate constant and I_a must be expressed. Kinetic constant is proportional with I_a at low light intensity[63,70] and $I_a^{0.5}$ at high light intensity.[71,72] Generally, $k \propto I_a^\beta$,[30,73] in which β is named an exponential effect factor of light intensity.

Effect of other factors

Effect of catalytic particle size. The smaller photocatalyst size was more favorable photoactivity toward PCD because of enhancing the number of active sites.[74] In the range from 58.2 nm to 150.2 nm of spherical CeO$_2$ particle size for the PCD of rhodamine B, the experimental result obeys the PFO model with k_1 relating to $1/d_p$.[75] A similar trend was observed for the PCD of methylene blue with TiO$_2$.[76,77] Xu *et al.* reported that the PCD rate of methylene blue in suspended aqueous solution well complied with the PFO model with modified k_1 as a function of d_p, expressed in (26) for d_p from 12 nm to 49 μm.[77]

$$k_1 = -0.064 \ln d_p + 0.260 \tag{26}$$

Effect of dissolved oxygen. Dissolved oxygen can adsorb onto the photocatalyst surface and then trap electrons, preventing the recombination of hole–electron pairs and positively affecting PCD rate.[30,63] The non-competitive L–H model (eqn (27)) is commonly adopted for the adsorption of dissolved oxygen on the surface of TiO$_2$.[63,78] Moreover, the non-competitive adsorption between dissolved oxygen and organic compounds was confirmed in the literature.[78,79]

$$r_P \propto \frac{K_{O_2}[O_2]}{1 + K_{O_2}[O_2]} \tag{27}$$

Effect of temperature. Generally, reaction temperature slightly affects photocatalysis.[61] With increasing temperature, the adsorption capacity of photocatalysts increases, enhancing the PCD rate of organic compounds.[45] This finding is in line for orange G in the range of 20–50 °C,[21] indigo carmine in the range of 20–40 °C,[61] and rhodamine B in the range of 30–50 °C.[80] The relationship between the rate constant of PCD and temperature obeys the Arrhenius equation (eqn (28)). Unfortunately, the recombination of hole–electron pairs is also improved at higher temperatures.[81] Therefore, the suitable temperature for PCD of organic compounds needs to be determined from the experiment. As in an investigation by Chen and Hsu, the PCD rate of methylene blue reaches maxima at 50 °C in a temperature range from 0 to 70 °C.[45]

$$k(T) = k_0 \exp\left(-\frac{E_a}{R_g T}\right) \tag{28}$$

Effect of initial concentration of organic compound. Findings from various reports for a dilute solution revealed that PCD rate increases along with increasing $C_{P,0}$.[34,64,82,83] The recombination time of hole–electron pairs is very short (a few nanoseconds),[84] causing that photo-excited sites only react in a very narrow area. Therefore, a high $C_{P,0}$ enhances the collision probability between organic molecules and photo-excited sites.[61] This rule is accepted when $C_{P,0}$ is less than a critical concentration. Over this level, the light absorption of organic compounds significantly contributes to the attenuation of light intensity, resulting in a demotion of PCD rate.[55,65,85,86] Relationship (20) is typically applied to express an inverse proportion of $C_{P,0}$ and rate constant according to PFO model.

New approach for photocatalytic degradation kinetics

As above overview, various factors have been interested in investigating the kinetic of PCD of organic compounds. It notes that particle size, dissolved oxygen, and temperature are the initial set-up conditions for each experiment and are not changed over contact time. However, this is opposite to light intensity, which depends on contaminants concentration. Therefore, the light intensity may be a significant factor affecting PCD kinetics.[87]

In suspension, not all the catalyst particles are photo-excited due to stretching/preventing the light of other particles. The total amount of talent sites, which can be photo-excited to photoactive sites under radiation, is represented by an apparent concentration [·]. The [·] is a function of photocatalyst properties, initial concentration of photocatalyst, and considered as a constant for each experiment. Under illumination, a part of talent sites is photo-excited to photoactive sites, expressed over apparent concentration [*]$_0$. The [*]$_0$ depends on light intensity as an exponential function (29).

$$\frac{[*]_0}{[\cdot]} = k_g I_a^\beta = k_g I_0^\beta e^{-\beta \mu_S C_S} e^{-\beta \mu_P C_P} \tag{29}$$

The photoactive sites exist in a liquid solution with an abundant amount of water, resulting in an immediate reaction with water to form *OH. Therefore, $[*OH]_0 \approx [*]_0$. After photo-excitation, the mechanism of PCD is assumed over the following elementary reactions:

Water separation:

$$* + H_2O \xrightarrow{k_s} *OH + H^+ \qquad (r1)$$

Adsorption:

$$P + *OH \xrightarrow{k_a} P*OH \qquad (r2)$$

Desorption:

$$P*OH \xrightarrow{k_d} P + *OH \qquad (r3)$$

Degradation reaction:

$$P*OH \xrightarrow{k_r} Q + *, \; n\text{-order reaction} \qquad (r4)$$

Balance of photoactive sites:

$$[*OH] = [*]_0 - [P*OH] \qquad (30)$$

According to reaction rate law, it reveals expressions:

$$\frac{d[P*OH]}{dt} = k_a[*OH]C_P - k_d[P*OH] - k_r[P*OH]^n \qquad (31)$$

$$-\frac{dC_P}{dt} = k_a[*OH]C_P - k_d[P*OH] \qquad (32)$$

Eqn (30) and ordinary differential eqn (31) and (32) reveal a kinetic model for PCD with variations C_P and $[P*OH]$ as a function of time. The PCD can be distinguished into two particular cases: (i) the rate of degradation reaction is significantly faster than the adsorption rate, and (ii) *vice versa*.

The rate of degradation is significantly faster than the rate of adsorption

In this case, all of P adsorbed onto *OH speedy change to product Q. Therefore, $[P*OH]$ is near zero, resulting $[*OH] \approx [*]_0$ from (30) and eqn (32), can be rewritten:

$$-\frac{dC_P}{dt} = k_a[*]_0 C_P \qquad (33)$$

In combining with (29), eqn (34) is obtained.

$$-\frac{dC_P}{dt} = k_a k_g[\cdot] I_0^\beta e^{-\beta \mu_S C_S} e^{-\beta \mu_P C_P} C_P = k_{1,ap} e^{-\beta \mu_P C_P} C_P \qquad (34)$$

where $k_{1,ap} = k_a k_g[\cdot] I_0^\beta e^{-\beta \mu_S C_S}$

If $C_P \ll 1$, $e^{-\mu_P C_P}$ is near 1. The simplified form (35) can be obtained from (34).

$$-\frac{dC_P}{dt} = k_{1,ap} C_P \qquad (35)$$

The eqn (35) for the PCD matches the PFO model.

Although the PFO model (eqn (35)) has been accepted for describing the kinetic of PCD, it may be inaccurate in some cases. Numerical solutions of eqn (34) (solid plots) and the PFO model (discrete points) were figured out for varying $C_{P,0}$, μ_P, $k_{1,ap}$, β and shown in Fig. 1 and S1†. The difference between the PFO and eqn (34) results is contributed by the light attenuation due to the contaminant's absorbance, represented through the term of $e^{-\beta \mu_P C_P}$.

The apparent rate constant ($k_{1,ap}$) and exponential effect factor of light intensity (β) barely affect the difference between the PFO and eqn (34) model, as presented in Fig. S1.† However, this difference is more significant with an increase in the initial concentration ($C_{P,0}$) and attenuation coefficient (μ_P), as presented in Fig. 1, in which the $C_{P,0}$ is more considerable than. For small $C_{P,0}$ (<0.01 mol L^{-1}) and μ_P (<2 L mol^{-1}), the solid line of eqn (34) also matches the dash-dot line of the PFO model, which proves the similarity of eqn (34) of the PCD with the PFO model. It means the contaminant's light absorbance is a faint contribution to the PCD kinetic. Similar comparison works were also built to apply for PCD of various organic compounds such as tetracycline,[88] rhodamine B,[40] methylene blue, and congo red.[89] At low $C_{P,0}$, good fits of the PFO to experimental kinetic data presented for PCD of tetracycline ($C_{P,0}$ = 0.11 mmol L^{-1}) on Fe-doping g-C$_3$N$_4$,[88] rhodamine B ($C_{P,0}$ = 0.01 mmol L^{-1}) on TiO$_2$ supported porous ceramic.[40] For PCD of methylene blue on flower-like titanium nano-particle, the compatibility between the experimental result and the PFO model was weaker with an increase in $C_{P,0}$ through the reduction of R^2 value from 0.9953 down to 0.9664 corresponding to $C_{P,0}$ from 0.03 up to 0.22 mmol L^{-1}.[90] Qu *et al.* studied the PCD of methylene blue and congo red on photocatalytic nanoparticles derived from marine clam shells.[89] The R^2 values from fitting the PFO model with experimental result were found to be 0.953 and 0.921 for methylene blue at $C_{P,0}$ = 0.24 and 0.031 mmol L^{-1}, and 0.986 and 0.856 for congo red at $C_{P,0}$ = 0.11 and 0.14 mmol L^{-1}, respectively. The weaker compatibility of the PFO model for PCD of congo red compared to methylene blue at the lower range of $C_{P,0}$ might be due to the stronger UV light absorption of congo red.[91,92]

The rate of degradation is very lower than the rate of adsorption

Because of degradation reaction at a slow rate, adsorption–desorption equilibrium of P on *OH can be achieved, resulting $\frac{d[P*OH]}{dt} = 0$. Therefore, eqn (36) is obtained from the rearranging of eqn (31).

$$k_a[*OH]C_P - k_d[P*OH] = k_r[P*OH]^n \qquad (36)$$

Value of $[*OH]$ can be calculated from eqn (30) and substituted to (36).

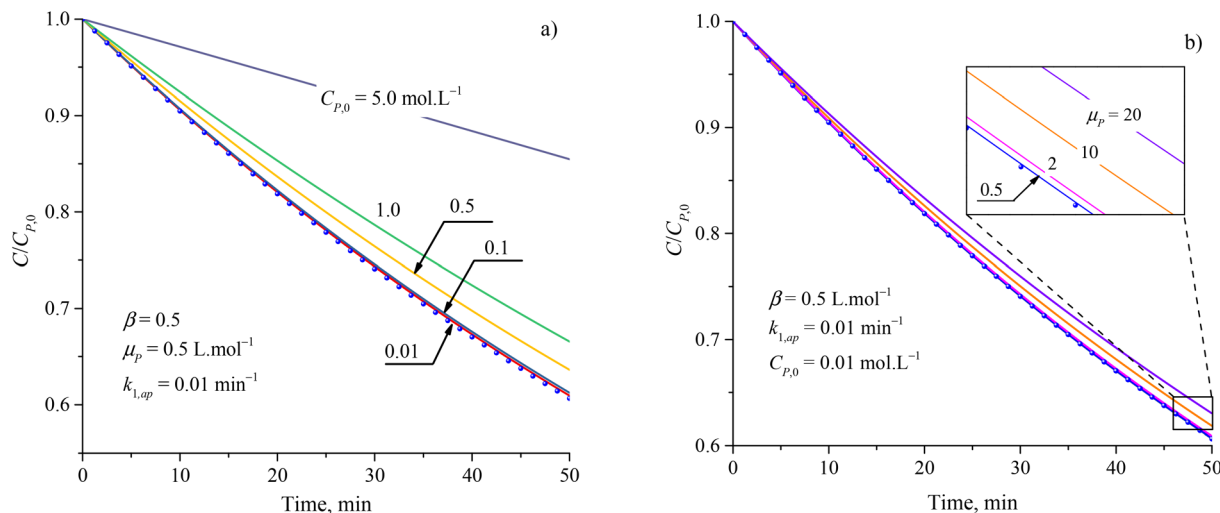$$k_a([*]_0 - [P*OH])C_P - k_d[P*OH] = k_r[P*OH]^n \qquad (37)$$

Fig. 1 Difference between results from the PFO model (discrete points) and eqn (34) (solid plots) at varied parameters of (a) initial concentration and (b) attenuation coefficient.

Manipulating (36) to (32), we obtain

$$-\frac{dC_P}{dt} = k_r[P^*OH]^n \tag{38}$$

✓ If $n = 0$, PCD exhibits a pseudo-zero-order kinetic model.

$$-\frac{dC_P}{dt} = k_r \tag{39}$$

✓ If $n = 1$, the apparent concentration of P*OH can be obtained from (37):

$$[P^*OH] = \frac{k_a[^*]_0 C_P}{k_d + k_r + k_a C_P} \tag{40}$$

And eqn (38) becomes:

$$-\frac{dC_P}{dt} = \frac{k_r k_a[^*]_0 C_P}{k_d + k_r + k_a C_P} = \frac{k_r k_a k_g[\cdot]I_0^\beta e^{-\beta\mu_S C_S} e^{-\beta\mu_P C_P} C_P}{k_d + k_r + k_a C_P} \tag{41}$$

Devising (41) through $(k_d + k_r)$:

$$-\frac{dC_P}{dt} = \frac{\frac{k_r k_a k_g[\cdot]I_0^\beta e^{-\beta\mu_S C_S}}{k_d + k_r} e^{-\beta\mu_P C_P} C_P}{1 + \frac{k_a}{k_d + k_r} C_P} = \frac{K_A e^{-\beta\mu_P C_P} C_P}{1 + K_B C_P} \tag{42}$$

with $K_A = \dfrac{k_r k_a k_g[\cdot]I_0^\beta e^{-\beta\mu_S C_S}}{k_d + k_r}$ and $K_B = \dfrac{k_a}{k_d + k_r}$.

A minor case for $C_P \ll 1$, $e^{-\mu_P C_P}$ is near 1. Eqn (42) can be simplified to (43).

$$-\frac{dC_P}{dt} = \frac{K_A C_P}{1 + K_B C_P} \tag{43}$$

Eqn (43) is uniform with the L–H model (10).

To evaluate the closeness of the L–H model and eqn (42), the numerical solutions for these models were found and shown in Fig. 2 for varying $C_{P,0}$, μ_P, and in Fig. S2† for varying K_A, K_B and β. As presented in Fig. S2a and b,† the discrepancies between the two models was maintained with increasing K_A and K_B. It indicates that the contaminant's light absorption cause an unchanged difference between the two models. It notes that $K_B = \dfrac{k_a}{k_d + k_r} \approx \dfrac{k_a}{k_d}$ represents the adsorption equilibrium. A large K_B ($k_a \gg k_d$) represents the irreversible adsorption (chemical adsorption) and a small K_B ($k_a \ll k_d$) represents the reversible adsorption (physical adsorption) of organic compound on a photocatalyst surface. The result indicates that both the L–H model and eqn (42) can be applied to all types of adsorption. The variation of β affects the match of the L–H model and eqn (42) (Fig. S2c†) insignificantly.

Fig. 2a and b show more differences between the solutions of the L–H model and eqn (42) in increasing $C_{P,0}$ and μ_P. For small $C_{P,0}$ (<0.01 mol L^{-1}) and μ_P (<0.1 L mol^{-1}), the two models are in better agreement. Study on PCD of metsulfuron-methyl on TiO$_2$ photocatalyst, Kim *et al.* showed that the L–H model reduced in compatibility with the experimental result through $R^2 = 0.942$ for $C_{P,0} = 0.052$ mmol L^{-1} and $R^2 = 0.905$ for $C_{P,0} = 0.131$ mmol L^{-1}.[93] As this trend applied for PCD of dye Auramine O on ZnO photocatalyst, $R^2 = 0.9594$ for $C_{P,0} = 0.13$ mmol L^{-1} and $R^2 = 0.5457$ for $C_{P,0} = 0.53$ mmol L^{-1}.[94] The contribution of the contaminant's light absorption to the L–H kinetic was discussed by Lilov *et al.*[95] However, this group did not investigate different $C_{P,0}$ values. Alvarez-Ramirez *et al.* also concluded that the L–H model is inappropriate for describing the PCD kinetic in a high range of reactant concentration.[19] In fact, it is rare for publications to show the results of processing PCD kinetic data according to the L–H model.
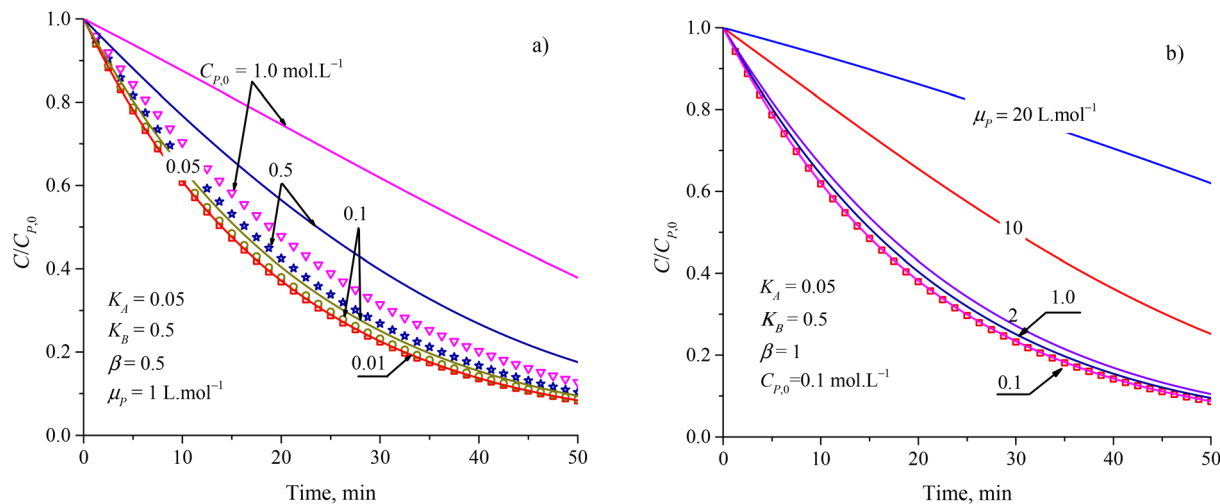
✓ If $n = 2$, solve (37) to obtain [P*OH].

Fig. 2 Difference between results from the L–H model (discrete points) and eqn (42) (solid plots) at varied parameters of (a) initial concentration and (b) attenuation coefficient.

$$[P*OH] = \frac{-(k_a C_P + k_d) + \sqrt{(k_a C_P + k_d)^2 + 4 k_a k_r [*]_0 C_P}}{2 k_r} \quad (44)$$

Substituting (44) into (38) with $n = 2$ to get:

$$-\frac{dC_P}{dt} = \frac{\left\{ -(k_a C_P + k_d) + \sqrt{(k_a C_P + k_d)^2 + 4 k_a k_r [*]_0 C_P} \right\}^2}{4 k_r} \quad (45)$$

Approximating a square root for (45)[96] to achieve a simplified equation:

$$\sqrt{(k_a C_P + k_d)^2 + 4 k_a k_r [*]_0 C_P} \approx k_a C_P + k_d + \frac{4 k_a k_r [*]_0 C_P}{2(k_a C_P + k_d)} \quad (46)$$

Therefore, eqn (45) becomes:

$$-\frac{dC_P}{dt} = \frac{1}{4 k_r} \left\{ \frac{2 k_a k_r [*]_0 C_P}{k_a C_P + k_d} \right\}^2 = k_r \left\{ \frac{k_a [*]_0 C_P}{k_a C_P + k_d} \right\}^2 \quad (47)$$

Substituting (29) into (47) to obtain:

$$-\frac{dC_P}{dt} = k_r \left\{ \frac{k_g [\cdot] I_0^\beta e^{-\beta \mu_S C_S} e^{-\beta \mu_P C_P} C_P}{k_d/k_a + C_P} \right\}^2 = k_{2,ap} \left(\frac{e^{-\beta \mu_P C_P} C_P}{k_H + C_P} \right)^2 \quad (48)$$

where $k_{2,ap} = k_r (k_g [\cdot] I_0^\beta e^{-\beta \mu_S C_S})^2$ and $k_H = \dfrac{k_d}{k_a}$.

A minor case for $C_P \ll 1$, $e^{-\beta \mu_P C_P}$ is nearly 1 and $C_P \ll k_H$. Eqn (49) is an approximate form of (48), known as the PSO model.

$$-\frac{dC_P}{dt} = \frac{k_{2,ap}}{k_H^2} C_P^2 = k'_{2,ap} C_P^2 \quad (49)$$

The increase of rate constants $k_{2,ap}$ and the decrease of k_H led to a faster decrease of $C/C_{P,0}$ as shown in Fig. S3a and b.† But the

difference between the results from the PSO model and eqn (48) is almost independent of the variation of $k_{2,ap}$ vs. k_H. Notably, $k_H = k_d/k_a$ is related to the adsorption type. The difference between the PSO model and eqn (48) is unchanged with the variation of k_H constant. As a result, both the PSO model and eqn (48) can be applied for the physical and chemical adsorption in the PCD process. Fig. S3c† presents virial discrepancies between the solutions for the eqn (48) at $\beta = 0.5$ and $\beta = 1$. Through the discussion mentioned, it can be seen that varying the values of β didnot have much effect on the compatibility between the PSO and eqn (48).

The approximation of the PSO model to eqn (48) is significantly unacceptable with a large $C_{P,0}$ and μ_P, as shown in Fig. 3. This result suggests that the PSO model cannot be used to describe the kinetics of PCD at a high solute concentration (high $C_{P,0}$) or the solute has good light absorption (high μ_P). At low $C_{P,0}$ (0.057, 0.086, and 0.115 mmol L^{-1}), the PCD kinetic of congo red on NiS nanoparticles was well described according to the PSO model with high R^2 (0.9986, 0.9982, and 0.9987).[37] For PCD of methyl orange on borohydride-reduced Fe reported by Shahwan et al., the experimental kinetic data followed the PSO model with $R^2 = 0.9771$ at $C_{P,0} = 0.03$ mmol L^{-1} and $R^2 = 0.9737$ at $C_{P,0} = 0.3$ mmol L^{-1}.[97]

Overall, the kinetics of the PCD process for organic compounds are affected by the absorbance of dissolved contaminants through the exponential effect factor of light intensity (β), attenuation coefficient (μ_P), and concentration. At low concentrations, the general equation for each case can be simplified. The curves of $C/C_{P,0}$ vs. time from the simplified model are always steeper than those from the general equations. The discrepancies between the simplified models and general equations barely change with variations of the apparent rate constant and β, but become more significant with rising concentration and μ_P. Although evidence for the concentration's effect on these discrepancies was demonstrated in the literature,
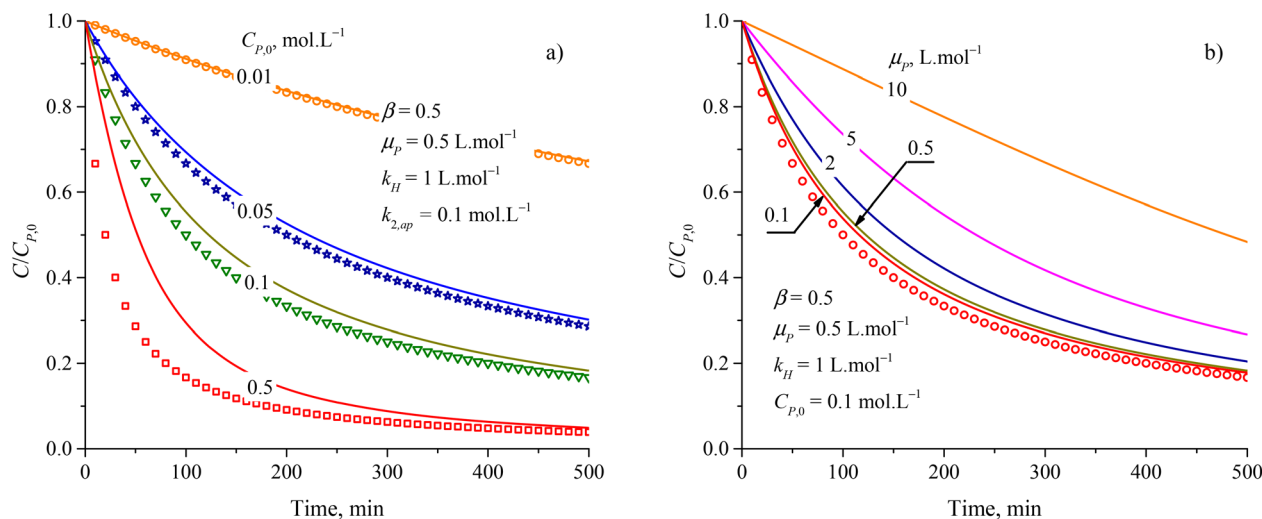
Fig. 3 Deference between results from the PSO model (discrete points) and eqn (48) (solid plots) at varied parameters of (a) initial concentration and (b) attenuation coefficient.
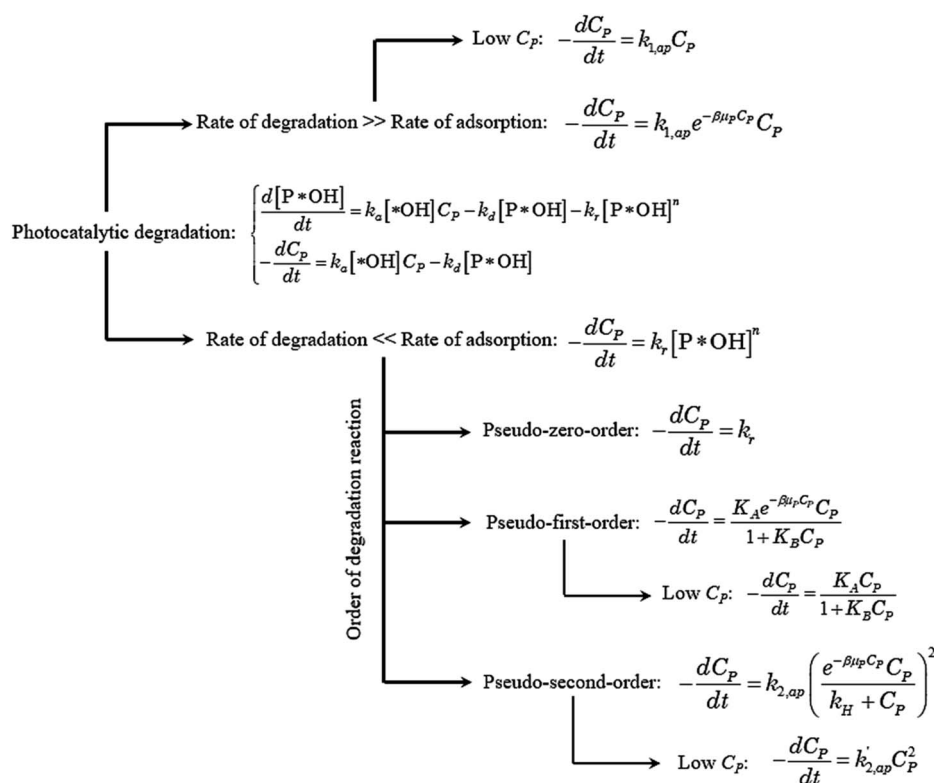

Fig. 4 Kinetic model flowchart of photocatalytic degradation in aqueous solution.

the effect of μ_P on PCD kinetics has not been explored. The summary of the obtained models is presented in Fig. 4.

Conclusions

The mechanism and characteristics of PCD can be explored through kinetic studies. Common kinetic models of PCD were reviewed, giving some limits and remarks for application in different experimental conditions. The effects of various factors on PCD kinetic, such as catalytic particle size, dissolved oxygen, temperature, initial concentration, and light intensity, are also discussed. Based on previous reports, elementary reactions in the PCD process are proposed, including the effect of light intensity. It found that the kinetic models of PCD are in ordinary differential equations. In low concentrations of

contaminants, simplified kinetic modes are a good match to the L–H and pseudo-order kinetic models.

Author contributions

Hai D. Tran drafted ideas, prepared draft models and designed the original structure of the manuscript. Dinh Quan Nguyen re-designed the manuscript, and calculated and discussed the approximation of equations/models with the literature. Phuong T. Do solved kinetic models. Uyen N. P. Tran overall reviewed and revised the manuscript.

Conflicts of interest

There are no conflicts to declare.

Acknowledgements

References

1 S. F. Ahmed, M. Mofijur, S. Nuzhat, A. T. Chowdhury, N. Rafa, M. A. Uddin, A. Inayat, T. M. I. Mahlia, H. C. Ong, W. Y. Chia and P. L. Show, *J. Hazard. Mater.*, 2021, **416**, 125912.

2 B. Koul, D. Yadav, S. Singh, M. Kumar and M. Song, *Water*, 2022, **14**(21), 3542.

3 Y. Zhang, *J. Phys.: Conf. Ser.*, 2020, **1549**, 022040.

4 S. A. Mohammadi, H. Najafi, S. Zolgharnian, S. Sharifian and N. Asasian-Kolur, *Sci. Total Environ.*, 2022, **843**, 157026.

5 M. Zhang, Q. Shi, X. Song, H. Wang and Z. Bian, *Environ. Sci. Pollut. Res.*, 2019, **26**, 10457–10486.

6 N. K. Chaturvedi, *Appl. Water Sci.*, 2022, **12**, 173.

7 M. Thanavel, S. K. Kadam, S. P. Biradar, S. P. Govindwar, B.-H. Jeon and S. K. Sadasivam, *SN Appl. Sci.*, 2019, **1**, 97.

8 L. H. Q. Anh, U. P. N. Tran, P. V. G. Nghi, H. T. Le, N. T. B. Khuyen and T. D. Hai, *Chim. Techno Acta*, 2022, **9**(4), 20229416.

9 W. Shi, C. Hao, Y. Shi, F. Guo and Y. Tang, *Sep. Purif. Technol.*, 2023, **304**, 122337.

10 X. Wang and L. Zhang, *RSC Adv.*, 2018, **8**, 40632–40638.

11 E. Amaterz, A. Tara, A. Bouddouch, A. Taoufyq, B. Bakiz, A. Benlhachemi and O. Jbara, *Rev. Environ. Sci. Biotechnol.*, 2020, **19**, 843–872.

12 H. M. Nguyen, C. M. Phan, T. Sen and S. A. Hoang, *Desalin. Water Treat.*, 2016, **57**(31), 14379–14385.

13 G. Lyngsie, L. Krumina, A. Tunlid and P. Persson, *Sci. Rep.*, 2018, **8**, 10834.

14 P. Attri, Y. H. Kim, D. H. Park, J. H. Park, Y. J. Hong, H. S. Uhm, K.-N. Kim, A. Fridman and E. H. Choi, *Sci. Rep.*, 2015, **5**, 9332.

15 R. J. Baxter and P. Hu, *J. Chem. Phys.*, 2002, **116**, 4379.

16 A. Hagemeyer and A. Volpe, Materials: Catalysts, in *Reference Module in Materials Science and Materials Engineering*, ed. S. Hashmi, Elsevier, 2016, pp. 158–165.

17 T. S. van Erp, T. Trinh, S. Kjelstrup and K. S. Glavatskiy, *Front. Phys.*, 2013, **1**, 36.

18 H. Swenson and N. P. Stadie, *Langmuir*, 2019, **35**(16), 5409–5426.

19 J. Alvarez-Ramirez, R. Femat, M. Meraz and C. Ibarra-Valdez, *J. Math. Chem.*, 2016, **54**, 375–392.

20 K. V. Kumar, K. Porkodi and F. Rocha, *Catal. Commun.*, 2008, **9**(1), 82–84.

21 D. Tekin, T. Tekin and H. Kiziltas, *Sci. Rep.*, 2019, **9**, 17544.

22 M. Irani, T. Mohammadi and S. Mohebbi, *J. Mex. Chem. Soc.*, 2016, **60**(4), 218–225.

23 G. V. Morales, E. L. Sham, R. Cornejo and M. E. F. Torres, *Lat. Am. Appl. Res.*, 2013, **43**, 325–328.

24 S. Basha, C. Barr, D. Keane, K. Nolan, A. Morrissey, M. Oelgemöller and J. M. Tobin, *Photochem. Photobiol. Sci.*, 2011, **10**, 1014–1022.

25 X. Lin, M. Li, Y. Li and W. Chen, *RSC Adv.*, 2015, **5**, 105227–105238.

26 D. E. Ollis, *Front. Chem.*, 2018, **6**, 00378.

27 N. K. Razdan and A. Bhan, *Proc. Natl. Acad. Sci. U. S. A.*, 2021, **118**(8), e2019055118.

28 B. Serrano, M. Salaices, A. Ortiz and H. I. de Lasa, *Chem. Eng. Sci.*, 2007, **62**(18–20), 5160–5166.

29 G. Pirgholi-Givi, S. Farjami-Shayesteh and Y. Azizian-Kalandaragh, *Phys. B*, 2020, **578**, 411886.

30 M. Subramanian and A. Kannan, *Korean J. Chem. Eng.*, 2008, **25**, 1300–1308.

31 R. Di Capua, F. Offi and F. Fontana, *Eur. J. Phys.*, 2014, **35**, 045025.

32 D. J. Davies, M. Clancy, D. Lighter, G. M. Balanos, S. J. E. Lucas, H. Dehghani, Z. Su, M. Forcione and A. Belli, *J. Clin. Monit. Comput.*, 2017, **31**, 967–974.

33 M. S. F. A. Zamri and N. Sapawe, *Mater. Today: Proc.*, 2019, **19**(4), 1261–1266.

34 N. Riaz, M. Hassan, M. Siddique, Q. Mahmood, U. Farooq, R. Sarwar and M. S. Khan, *Environ. Sci. Pollut. Res.*, 2020, **27**, 2992–3006.

35 N. Barka, S. Qourzal, A. Assabbane and Y. Ait-Ichou, *J. Environ. Sci. Eng.*, 2010, **4**(5), 1–5.

36 F. A. Aisien, N. A. Amenaghawon and E. F. Ekpenisi, *J. Eng. Appl. Sci.*, 2013, **9**, 11–16.

37 H. Guo, Y. Ke, D. Wang, K. Lin, R. Shen, J. Chen and W. Weng, *J. Nanopart. Res.*, 2013, **15**, 1475.

38 R. Kumar, A. Kumar Singh and P. S. Mondal, *Mater. Today: Proc.*, 2022, **66**(7), 3244–3249.

39 J. Pan, L. Wang, Y. Shi, L. Li, Z. Xu, H. Sun, F. Guo and W. Shi, *Sep. Purif. Technol.*, 2022, **284**, 120270.

40 R. F. de M. Peters, P. A. M. dos Santos, T. C. Machado, D. A. R. Lopez, Ê. L. Machado and A. de A. L. Rodriguez, *Ecletica Quim. J.*, 2018, **43**(1), 26–32.

41 B. Liu, Y. Li, Y. Wu and S. Xing, *Chem. Eng. J.*, 2021, **417**, 127972.

42 P. Gharbani, A. Mehrizad and S. A. Mosavi, *npj Clean Water*, 2022, **5**, 34.

43 F. Guo, Z. Chen, X. Huang, L. Cao, X. Cheng, W. Shi and L. Chen, *Sep. Purif. Technol.*, 2021, **275**, 119223.

44 W. Shi, W. Sun, Y. Liu, K. Zhang, H. Sun, X. Lin, Y. Hong and F. Guo, *J. Hazard. Mater.*, 2022, **436**, 129141.

45 Y.-W. Chen and Y.-H. Hsu, *Catalysts*, 2021, **11**, 966.

46 J. K. Yang, S. M. Lee and M. S. Siboni, *Environ. Technol.*, 2012, **33**(17), 2027–2032.

47 M. Pavel, C. Anastasescu, R.-N. State, A. Vasile, F. Papa and I. Balint, *Catalysts*, 2023, **13**(2), 380.

48 D. Ollis, *Appl. Catal., B*, 2017, **209**, 174–182.

49 G. Rytwo and A. L. Zelkind, *Catalysts*, 2022, **12**, 24.

50 M. A. Mahmoud, A. Poncheri, Y. Badr and M. G. Abd El Wahed, *S. Afr. J. Sci.*, 2009, **105**, 299–303.

51 C. N. Rani, *Water Pract. Technol.*, 2022, **17**(1), 517–528.

52 C. M. Ling, A. R. Mohamed and S. Bhatia, *Chemosphere*, 2004, **57**(7), 547–554.

53 A. Spence, D. J. Worth and S. T. Kolaczkowski, *Comput. Chem. Eng.*, 1995, **19**(11), 1169–1171.

54 L. Ernawati, A. W. Yusariarta, A. D. Laksono, R. A. Wahyuono, H. Widiyandari, R. Rebeka and V. Sitompu, *J. Phys.: Conf. Ser.*, 2021, **1726**, 012017.

55 N. N. Bahrudin, *Appl. Surf. Sci. Adv.*, 2022, **7**, 100208.

56 I. Ahmad, Q. Fasihullah and F. H. M. Vaid, *J. Photochem. Photobiol., B*, 2006, **82**(1), 21–27.

57 P. K. Sanoop, S. Anas, S. Ananthakumar, V. Gunasekar, R. Saravanan and V. Ponnusami, *Arabian J. Chem.*, 2016, **9**(2), S1618–S1626.

58 C. L. Wang, *J. Adv. Dielectr.*, 2011, **8**(5), 1850034.

59 T. R. Sahoo and B. Prelot, Adsorption processes for the removal of contaminants from wastewater: the perspective role of nanomaterials and nanotechnology, in *Nanomaterials for the Detection and Removal of Wastewater Pollutants*, ed. B. Bonelli, F. Freyria, I. Rossetti and R. Sethi, Elsevier, 2020, pp. 162–222.

60 R. Molinari, A. Caruso and L. Palmisano, *Photocatalytic Processes in Membrane Reactors, in Catalytic Membranes and Membrane Reactors*, ed. J. G. S. Marcano and T. T. Tsotsis, Elsevier B.V., 2010, pp. 166–189.

61 N. Barka, A. Assabbane, A. Nounah and Y. A. Ichou, *J. Hazard. Mater.*, 2008, **152**(3), 1054–1059.

62 D. Ollis, C. G. Silva and J. Faria, *Catal. Today*, 2015, **240**, 80–85.

63 N. Daneshvar, M. Rabbani, N. Modirshahla and M. A. Behnajady, *J. Photochem. Photobiol., A*, 2004, **168**(1–2), 39–45.

64 D. Y. Murzin, *Catal. Commun.*, 2008, **9**(9), 1815–1816.

65 K. M. Reza, A. Kurny and F. Gulshan, *Appl. Water Sci.*, 2017, **7**, 1569–1578.

66 M. A. Abdelrhman, *Estuaries Coasts*, 2017, **40**, 994–1012.

67 T. A. Egerton, *Molecules*, 2014, **19**(11), 18192–18214.

68 W. Baran, A. Makowski and W. Wardas, *Dyes Pigm.*, 2008, **76**(1), 226–230.

69 T. G. Mayerhöfer, S. Pahlow and J. Popp, *ChemPhysChem*, 2020, **21**(18), 2029–2046.

70 M. W. Peterson, J. A. Turner and A. J. Nozik, *J. Phys. Chem.*, 1991, **95**(1), 221–225.

71 D. Bahnemann, D. Bockelmann and R. Goslich, *Sol. Energy Mater.*, 1991, **24**(1–4), 564–583.

72 C. Kormann, D. W. Bahnemann and M. R. Hoffmann, *Environ. Sci. Technol.*, 1991, **25**(3), 494–500.

73 D. Chen and A. K. Ray, *Water Res.*, 1998, **32**(11), 3223–3234.

74 D. Zhang, S. Lv and Z. Luo, *RSC Adv.*, 2020, **10**, 1275–1280.

75 Z. Cui, L. Zhang, Y. Xue, Y. Feng, M. Wang, J. Chen, B. Ji, C. Wang and Y. Xue, *Int. J. Miner., Metall. Mater.*, 2022, **29**, 2221–2231.

76 C. Retamoso, N. Escalona, M. González, L. Barrientos, P. Allende-González, S. Stancovich, R. Serpell, J. L. G. Fierro and M. Lopez, *J. Photochem. Photobiol., A*, 2019, **378**, 136–141.

77 N. Xu, Z. Shi, Y. Fan, J. Dong, J. Shi and M. Z.-C. Hu, *Ind. Eng. Chem. Res.*, 1999, **38**(2), 273–279.

78 C. S. Turchi and D. F. Ollis, *J. Catal.*, 1990, **122**(1), 178–192.

79 N. K. Youn, J. E. Heo, O. S. Joo, H. Lee, J. Kim and B. K. Min, *J. Hazard. Mater.*, 2010, **177**(1–3), 216–221.

80 M. Siddique, N. M. Khan and M. Saeed, *Z. Phys. Chem.*, 2019, **233**(5), 595–607.

81 Y. Wang and R. Long, *ACS Appl. Mater. Interfaces*, 2019, **11**(35), 32069–32075.

82 J. C. García-Prieto, L. A. González-Burciaga, J. B. Proal-Nájera and M. García-Roig, *Catalysts*, 2022, **12**, 122.

83 M. Abbas, *J. Chem. Res.*, 2021, **45**(7–8), 694–701.

84 F. Chen, T. Ma, T. Zhang, Y. Zhang and H. Huang, *Adv. Mater.*, 2021, **33**(10), 2005256.

85 S. H. Borji, S. Nasseri, A. H. Mahvi, R. Nabizadeh and A. H. Javadi, *J. Environ. Health Sci. Eng.*, 2014, **12**, 101.

86 L. Bobirică, C. Bobirică, G. I. Lupu and C. Orbeci, *Appl. Sci.*, 2021, **11**, 11664.

87 X. Zhan, C. Yan, Y. Zhang, G. Rinke, G. Rabsch, M. Klumpp, A. I. Schäfer and R. Dittmeyer, *React. Chem. Eng.*, 2020, **5**, 1658–1670.

88 H. Sun, L. Wang, F. Guo, Y. Shi, L. Li, Z. Xu, X. Yan and W. Shi, *J. Alloys Compd.*, 2022, **900**, 163410.

89 T. Qu, X. Yao, G. Owens, L. Gao and H. Zhang, *Sci. Rep.*, 2022, **12**, 2988.

90 F. H. Mustapha, A. A. Jalil, M. Mohamed, S. Triwahyono, N. S. Hassan, N. F. Khusnun, C. N. C. Hitam, A. F. A. Rahman, L. Firmanshah and A. S. Zolkifli, *J. Cleaner Prod.*, 2017, **168**, 1150–1162.

91 N. Ali, A. Said, F. Ali, F. Raziq, Z. Ali, M. Bilal, L. Reinert, T. Begum and H. M. N. Iqbal, *Water, Air, Soil Pollut.*, 2020, **231**, 50.

92 T.-J. Whang, H.-Y. Huang, M.-T. Hsieh and J.-J. Chen, *Int. J. Mol. Sci.*, 2009, **10**(11), 4707–4718.

93 S.-H. Kim, H. H. Ngo, H. K. Shon and S. Vigneswaran, *Sep. Purif. Technol.*, 2008, **58**(3), 335–342.

94 K. V. Kumar, K. Porkodi and A. Selvaganapathi, *Dyes Pigm.*, 2007, **75**(1), 246–249.

95 E. Lilov, V. Lilova, S. Nedev, S. Kozhukharov and C. Girginov, *J. Chem. Technol. Metall.*, 2022, **57**(6), 1175–1182.

96 D. Fowler and E. Robson, *Hist. Math.*, 1998, **25**(4), 366–378.

97 T. Shahwan, S. A. Sirriah, M. Nairat, E. Boyacı, A. E. Eroğlu, T. B. Scott and K. R. Hallam, *Chem. Eng. J.*, 2011, **172**(1), 258–266.